# Molecular Dynamics Investigation on Thermal Conductivity and Phonon Transmission of Folded Graphene

**Jian Gao,**[1,2] **Chao Si,**[3,z] **Yan-Ru Yang,**[1] **Bing-Yang Cao,**[4] **and Xiao-Dong Wang**[1,2,z]

[1]*State Key Laboratory of Alternate Electrical Power System with Renewable Energy Sources, North China Electric Power University, Beijing 102206, People's Republic of China*
[2]*Research Center of Engineering Thermophysics, North China Electric Power University, Beijing 102206, People's Republic of China*
[3]*Institute of Energy and Power Engineering, Zhejiang University of Technology, Hangzhou 310023, People's Republic of China*
[4]*Key Laboratory for Thermal Science and Power Engineering of Ministry of Education, Department of Engineering Mechanics, Tsinghua University, Beijing 100084, People's Republic of China*

This work employs the molecular dynamics approach to investigate effects of folding on thermal conductivity of graphene that contains 86 × 60 atoms, to provide the phononics understanding for thermal conductance modulator devices constituted by the folded graphene. The spectral energy density method is utilized to perform phononics analyses. It is found that the folding significantly reduces the contribution of the TA-phonon to the thermal conductivity, so that the thermal conductivity of folded graphene is 64.42% of the one before folding. The phonon dispersion curves are analyzed to quantify the TA-phonon transmission before and after folding. It turns out that the TA-phonon lifetime of the graphene, averaging 7.57 ps before folding, is significantly reduced and only remains 4.27 ps after folding. The effects of the stress contribution and phonon mode mismatch behavior are discussed to understand how the folding affects the TA-phonon transmission. It is found that the effects of stress on the TA branch phonon transmission and the thermal conductivity are negligible. While the phonon-folding scattering should be responsible for the reduced lifetime and the decreasing thermal conductivity for folded graphene. When the phonons pass the fold, some phonons along the in-plane direction need to change from the in-plane mode into a mixed mode, and change back to an in-plane mode after passing the fold.

Graphene, the one-atom-thick planar sheet of $sp^2$ carbon atoms that are arranged by honey-comb crystal lattice, has a wide range of practical applications in nano-devices,[1] batteries[2] and composite materials.[3] The fantastic thermal and electrical properties of graphene and its derived nanostructures also attract many attentions of scientists in the last few years.[4–6] There is an important role that graphene's derived nanostructures can play is the so-called thermal conductance modulator (TCM) in nano-scale thermal management, which can perform similar operations as the rheostat in electronic circuits.[7,8] After attempting numerous but unsatisfactory efforts via the treatments of defects,[9] impurities,[10,11] and edge chirality,[12] the strategy of folded graphene provide a hopeful way to realize the application of nano-scale TCM, through varying the folded angle and the inter-layer distance of graphene. Inspired by this strategy, as shown in Table I, Ju et al.[13] treat the folded graphene as a heat conduction module when designing the nano-scale TCM devices, and the thermal properties are studied. The electronic properties of the folded graphene are also investigated by Yin et al.[14] and Chang et al.,[15] and the information about the energy gaps are received attentions in their work. Physically, the heat carrier in graphene, phonon, dominates the in-plane heat conduction through the graphene. Consequently, applying the strategy of folded graphene as nano-scale TCM is definitely unreliable unless the rules associated with the thermal conductivity are perfectly revealed and the related phononics problems are settled.

The folding process can achieve continuously adjustable thermal conductivity of graphene, so that the pioneering work of Ouyang et al.[8] pays attention to the quantitative relationship between the folding parameters and the thermal conductivities of the folded graphene. Table II presents the efforts[7,8,16] to obtain the relationship and the phononics mechanism behind it. In the letter of Ouyang et al.,[8] however, the phonon transmission in the folded graphene are

rarely discussed. Later, to explain how folding affects the thermal conductivity of graphene, Yang's group[7,16] studies the folded graphene with various shape parameters. Their earlier work[16] investigates the effect of the number of folds and the folding pressure. The phononics analysis of the entire folded graphene are carried out using the transmission spectra calculation. Strictly, it is hard to tell the individual function of the fold, for the phonon properties in Ref. 16 are calculated in the entire folded graphene. In their latter work,[7] a new phonon scattering regime, named by phonon-folding scattering, is firstly introduced. For the folded graphene, most of the deformations of the original honey-comb crystal lattice happen in the fold region, while the other parts of the folded graphene almost remain flat. Consequently it is a brilliant idea that dividing the folded graphene into the two parts (the fold region and the plane region), and then trying to analyze the phonon scattering which is strongly dependent on the partial structure of the fold region. Besides, they speculate that the major inducement of the phonon-folding scattering is the exchange between the in-plane mode and the out-of-plane mode. Their density of spectral (DOS) calculation provide some evidences to the speculation. Unfortunately, questions still remain about the relationship between the phonon-folding scattering and the thermal conductivity. In the classic DOS calculation, detail phononics characteristics of the phonon-folding scattering is not comprehensive enough. For example, although DOS conclusion can figure out the in-plane mode and the out-of-plane of phonon, it can neither accurately predict the characteristics of the phonon branches, nor deeply analyze the phonon contribution rate. Hence, how and why the folding affects the phonon branches are still open questions. Otherwise, the folded graphene studied by Yang's group[7,16] contains a few number of folds, so that the questions should be too complicated to answer because the structures of every folds could be different. To reveal the role played by the fold region in the phonon-folding scattering, the folded graphene which only contains one fold deserves deeply investigations using the phononics approach.

[z]E-mail: sic2018@zjut.edu.cn; wangxd99@gmail.com

**Table I. Literature that investigate the thermal and electronic properties of the folded graphene.**

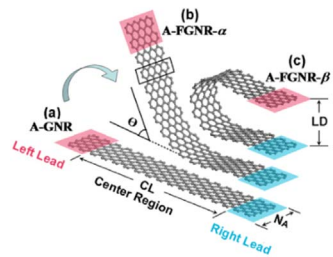| Author and reference | Schematic structure | Studied property | Major conclusion |
|---|---|---|---|
| Ju[13] |  | Thermal property | (1) The thermal conductivity of folded graphene is reduced to 3.3% compared to its counterpart.<br><br>(2) The thermal conductivity calculated from heat flux arising from van der Waals interaction is much smaller than that from both the van der Waals and bonding interaction. |
| Yin[14] |  | Electronic property | (1) The folded graphene can be stable when it reaches its critical length.<br><br>(2) Upon folding, the band gap can be opened. |
| Chang[15] |  | Electronic property | (1) The interlayer interaction and hybridization of four orbitals on the curved surface lead to smaller energy gaps, anti-crossing bands.<br><br>(2) The folding energies in the AB or AA' stacking are lower.<br>(3) The energy gaps decrease with increased ribbon width. |

**Table II. Literature that investigate the relationship between the folding parameters and the thermal conductivities of the folded graphene.**
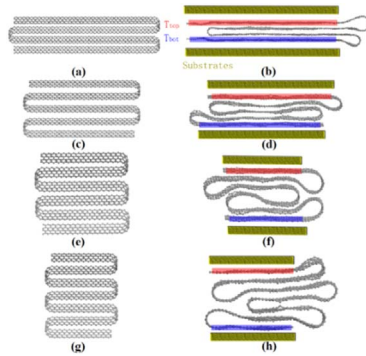
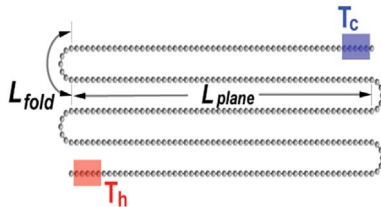| Author and reference | Schematic structure | Major conclusion |
|---|---|---|
| Ouyang[8] |  | (1) The thermal conductivity can be modulated through varying the geometric structures.<br><br>(2) The thermal conductance decreases linearly with the increasing of $\theta$, while that firstly increases and then decreases as the LD increases. |
| Yang[16] |  | (1) A detailed mechanism of modulating phonons by folds are presented.<br><br><br><br>(2) The thermal conductivity of folded graphene can be decreased up to 70% of its counterpart.<br>(3) The percentage of reduction is dependent on the number of the fold.<br>(4) The more the structure is compressed, the more the thermal conductance is reduced. |
| Song[7] |  | (1) An instantaneously adjustable thermal resistor based on folded graphene are proposed.<br><br><br>(2) The thermal resistivity in folded graphene depends linearly on the length between two folds.<br>(3) The underlying physical mechanism is phonon-folding scattering due to mismatch between the fold and plane. |

Although preparing nano-scale folded graphene in lab is not difficult, it is still hard to measure the thermal conductivity of the nano-scale folded graphene in experiment.[17] As traditional approaches to measure the thermal conductivity of the graphene, neither the Raman Optothermal method[5] nor the Electrical self-heating method[18] can avoid generating a huge heat wave inside the graphene. Hence, when they are employed to measure the thermal conductivity of the folded graphene, it is hard to maintain the stability of the folding structure of the folded graphene. Then an appropriate nano-scale simulation approach will be chosen to study the phonon-folding scattering.

In this work, molecular dynamics (MD) simulation[19–23] is utilized to simulate the folded graphene which contains one fold. The phonon transmission of the folded graphene is investigated by the spectral energy density (SED) approach.[24] As the comparison group, the bi-layer graphene (BLG) and single-layer graphene (SLG) are also studied using the same approach. To further clarify the role played by the fold region, the phonon dispersion relationship will be analyzed.

## Methods and Simulation Details

This work employs the Large-scale Atomic/Molecular Massively Parallel Simulator (LAMMPS®)[25] packages to perform the molecular dynamics (MD) simulations. The folded graphene will be built in the MD simulations, the thermal conductivity will be predicted, and the corresponding phononics analysis will be carried out.

The atomic structures built in the packages are shown in Fig. 1. The initial structure of the folded graphene shown in Figs. 1a and 1b consists of two parts, the semi-CNT region and the AA-stacking bilayer region. The in-plane sizes of the bilayer region are both 8.70 × 7.48 nm² with 2400 carbon atoms arranged by honey-comb crystal lattice. The edge in the $x$ direction is armchair. The semi-CNT region can be considered as half of a (3,3)-CNT which contains 180 atoms. Free boundary conditions are used in the $x$ and $z$ directions, and periodic boundary conditions are used in the $y$ direction. To prevent the formation of chemical bonds and close the

edges,[14] the edge atoms are saturated by hydrogen atoms. In the LAMMPS approach, the size of the simulation box is 30 × 8 × 20.4 nm³, which is much larger than the initial volume of folded graphene. The folded graphene is controlled to reach its relaxation equilibrium state under the NPT simulation at 300 K and 0 Pa for 5 ns, followed by an NVE simulation for another 5 ns. The velocity-Verlet algorithm is utilized, and the simulation time step is set as 0.5 fs. The AIREBO multibody potential model is used to model the atom interactions,[23] as described in the following equation[26]:

$$V_{ij} = V_{ij}^{REBO} + V_{ij}^{LJ} + \sum_{k \neq i,j} \sum_{l \neq i,j,k} V_{ijkl}^{TORSION} \qquad [1]$$

Where $V_{ij}^{REBO}$ is the bond energy of atoms $i$ and $j$ modeled by the REBO, $V_{ij}^{LJ}$ is the L-J potential term, and $V_{ijkl}^{TORSION}$ is the torsion term which describe the potential energy of a four-body torsion that depends on the dihedral angle. As shown in Figs. 1c and 1d, after the relaxation equilibrium period, the semi-CNT region forms a larger semicircle, which is denoted by the fold region. The thickness of the folded graphene is 0.458 nm. For convenience in the following discussion, the folded graphene is called AAFG for short. As comparisons, the SLG and the AA-stacking bilayer graphene (AABG for short) are also built in MD simulation shown in Fig. 2. The SLG shown in Figs. 2(a-1) and 2(a-2) contains 2400 atoms with the thickness of 0.34 nm. The periodic boundary conditions are adopted in all the $x, y, z$ directions. For the AABG shown in Figs. 2(b-1) and 2(b-2), the in-plane size is 8.70 × 7.48 nm², and each layer contains 2400 atoms. The bilayer region of the AAFG and the AABG almost have the same size. The boundary conditions are the same as the folded graphene, that is, free boundary conditions in the $x$ and $z$ directions and periodic boundary conditions in the $y$ direction. Figures 2(c-1) and 2(c-2) show the structure that fully unfolded by the above AAFG, or the unfold-AAFG. It can be easily speculated that the size of the unfold-AAFG is 18.26 × 7.48 nm², and it contains 5040 carbon atoms. In order to uncover the effect of the edge hydrogenation, a hydrogenated bilayer graphene (AABG-H) shown in Figs. 2(d-1) and 2(d-2) is also built in the MD
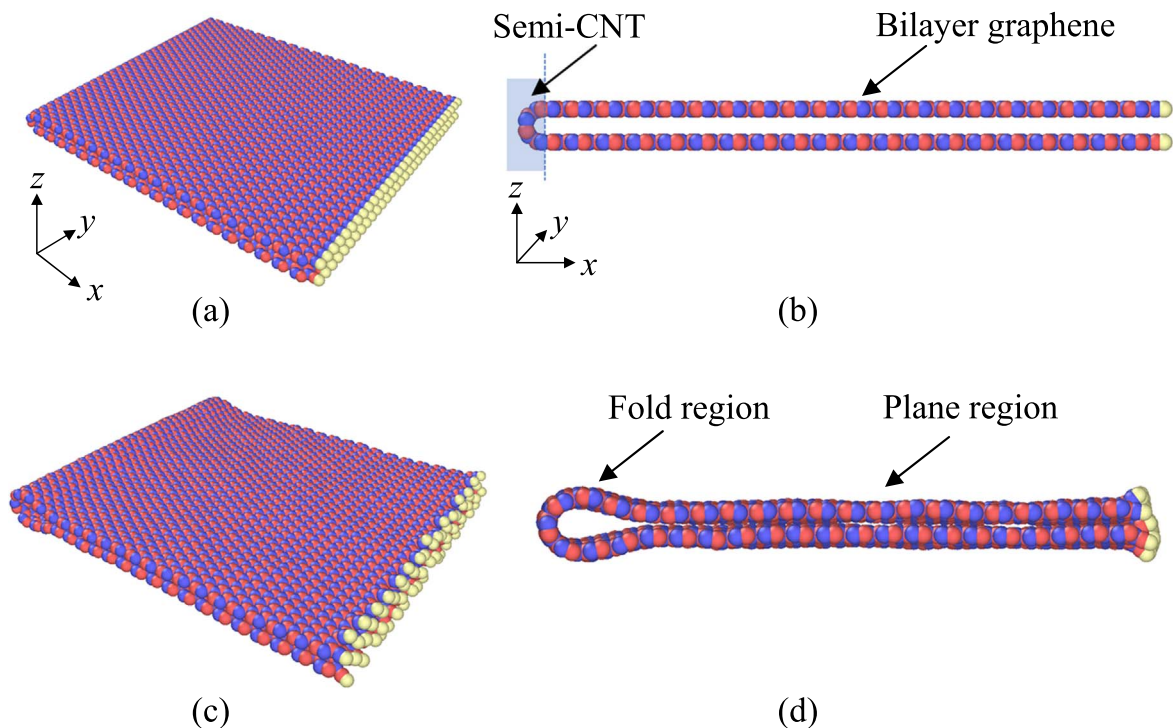


**Figure 1.** Schematic diagrams of folded graphene (AAFG for short) built in the packages. (a) 3-dimensional view and (b) side view of the initial structure, as well as (c) 3-dimensional view and (d) side view of the folded graphene after the relaxation equilibrium process.
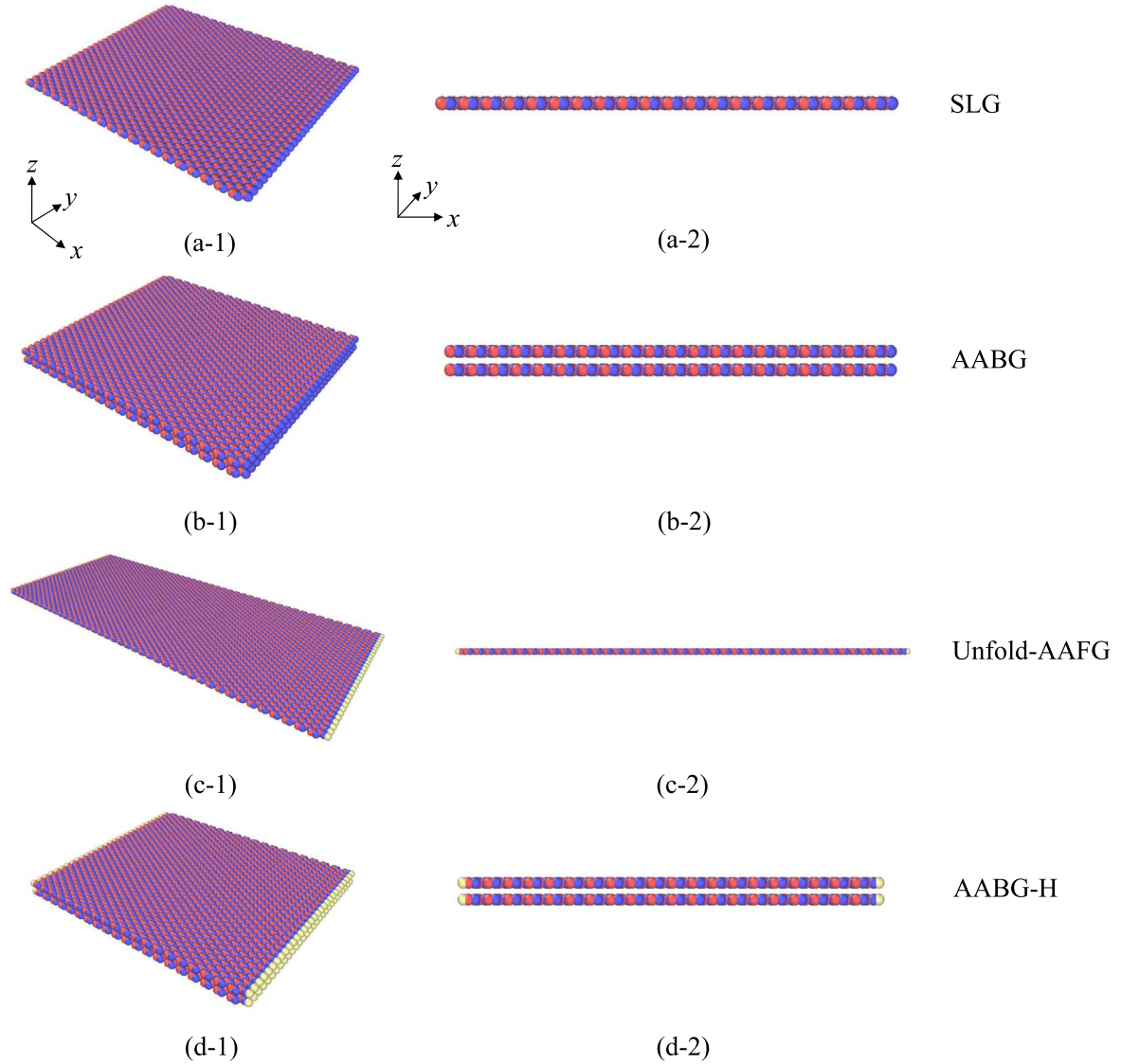
**Figure 2.** Schematic diagrams of the graphene as comparisons, (a-1) the 3-dimensional view and (a-2) the side view of single-layer graphene (SLG), (b-1) the 3-dimensional view and (b-2) the side view of bilayer graphene (AABG), (c-1) the 3-dimensional view and (c-2) the side view of Unfold-AAFG, as well as (d-1) the 3-dimensional view and (d-2) the side view of hydrogenated bilayer graphene (AABG-H).

approach. Its size and thickness are the same as AABG, $8.70 \times 7.48$ nm$^2$, while the boundary conditions are the same as AAFG, free boundary conditions in the $x$ and $z$ directions and periodic boundary conditions in the $y$ direction, due to the hydrogenation at both ends.

To predict the phonon thermal conductivities of the AAFG, AABG, Unfold-AAFG, AABG-H, and SLG, the characteristics of the phonon transmission and phonon collision can be predicted by Boltzmann transport equation under the relaxation time approximation, so that the phonon thermal conductivity can be expressed as[24]

$$\lambda = \sum_s \sum_\omega c_{ph} v_g^2 \tau \qquad [2]$$

Where $c_{ph}$ is the phonon specific heat, $v_g$ is the phonon group velocity, and $\tau$ is the phonon lifetime. It should be noted that the values of the phonon thermal conductivities are different from the experimentally measured thermal conductivities, due to the relaxation time approximation and the neglected quantum effects in the classic MD simulations.

To reveal the phonon properties of folded graphene, the spectral energy density (SED) method raised by McGaughey's group[27] was used to calculate the phonon dispersion relationship. The SED

formula $\Phi$ can be expressed as the relationship between the wave vector $\mathbf{q}$ and the frequency $\omega$, that is,

$$\Phi(\mathbf{q}, \omega) = \frac{1}{4\pi\tau_0 l} \sum_\alpha \sum_b m_b \left| \int_0^{\tau_0} \sum_l \dot{u}_\alpha(l, b) \exp(i\mathbf{q} \cdot \mathbf{r}(l, 0) - i\omega t) dt \right|^2$$

[3]

Where $m_b$ is the mass of the $b$ atom in the $l$th unit cell, $\dot{u}_\alpha(l, b)$ is the velocity of the atom $b$ in the $\alpha$ direction, $\tau_0$ is the total calculation time, and $\mathbf{r}(l, 0)$ is the equilibrium position of the $l$th unit cell. There will be some regions that contain specified peaks, and the phonon lifetime is obtained by fitting these peaks by Lorentzian function,

$$\Phi(\mathbf{q}, \omega) = \frac{I}{1 + ((\omega - \omega_c)/\gamma)^2} \qquad [4]$$

Where $I$ is the peak magnitude, $\omega_c$ is the frequency at the peak center, and $\gamma$ is width at half maximum. The phonon lifetime can be defined as $\tau = 1/2\gamma$, and the group velocity can be defined as $v_g = \partial\omega/\partial\mathbf{q}$. The value of the phonon specific heat $c_{ph}$ can be calculated by

the Einstein model under the harmonic approximation, as

$$c_{\text{ph}} = \frac{\left(\frac{\hbar\omega}{k_{\text{B}}T}\right)^2 e^{\frac{\hbar\omega}{k_{\text{B}}T}}}{(e^{\frac{\hbar\omega}{k_{\text{B}}T}} - 1)^2} \cdot \frac{k_B}{V} \qquad [5]$$

Where $k_{\text{B}}$ is Boltzmann constant, $V$ is the volume of the system, $T$ is the temperature, $\hbar$ is the reduced Planck constant. Therefore, the phonon thermal conductivity expressed in Eq. 2 now can be obtained by post-processing the MD simulation results. In the SED method, the phonon transmission in Γ-M direction will be predicted. Since the Γ-M direction is parallel to the armchair direction in graphene based on the structure of the First Brillouin Zone, the calculated phonon thermal conductivity is the $x$-component of the thermal conductivity.

### Results and Discussion

In this work, firstly, thermal conductivities of the $8.70 \times 7.48$ nm$^2$ AAFG with 5040 atoms will be predicted. Then, the phononics analysis will be carried out so that the effect of the folding on the phonon branches of graphene can be comprehensively obtained. Phonon dispersion relationship and phonon lifetime will be discussed to understand the role of folding played in the phonon-folding scattering. Finally, the stress distribution of the folded graphene will be showed and the phonon mode mismatch will be discussed. In all the above discussion, conclusions about SLG, AABG, Unfold-AAFG, and AABG-H will also be exhibited for the purpose of comparison.

*Thermal conductivity.*—EMD Simulations are performed at 300 K to predicted the thermal conductivities of the AAFG, AABG, Unfold-AAFG, AABG-H, and SLG, as shown in Fig. 3. The thermal conductivity of SLG at 300 K is 100.12 W m$^{-1}$ K$^{-1}$, which is much lower than the reported experimental value of 2500–5300 W m$^{-1}$ K$^{-1}$,[5,28] for the graphene length in this work is much shorter than the phonon mean free path. The thermal conductivity of AAFG is 44.52 W m$^{-1}$ K$^{-1}$. To verify the accuracy of this work, the ratio of the AAFG thermal conductivity to Unfold-AAFG is calculated as 44.52/68.76 = 0.647, and the ratio for the same characteristic parameter reported in Ref. 8 is 0.66. Moreover, it should be noted that the edge of the AAFG is hydrogen terminated compared with the SLG. The calculation of Evans et al.[12] has shown that H-terminated atoms at the edge of graphene has a significant effect on lowering thermal conductivity. To quantify the influence of H-terminated atoms, the thermal conductivity of the Unfold-AAFG as the comparison is also calculated, and the result is 68.76 W m$^{-1}$ K$^{-1}$. It can be confirmed that the thermal conductivity of graphene after folding is 64.7% of that before folding, which is consistent with the conclusion of Yang[16]: the thermal conductivity of folded graphene can be decreased up to 70% compared to its counterpart.

It is known that the thermal conductivity of graphene decreases with the increasing number of layers.[29] After the graphene is folded, there will be two parts, the fold region and the plane region. The thermal conductivities of AABG and AABG-H are calculated so that the effect of the two parts on heat conduction can be verified. For clarity, the thermal conductivity of AABG and AABG-H are 74.33 W m$^{-1}$ K$^{-1}$ and 58.83 W m$^{-1}$ K$^{-1}$, respectively. Both of them are higher than the thermal conductivity of the folded graphene, which indicates that the effect of the fold region is significant.

*Phonon contributions to the thermal conductivity.*—To understand the effect of the fold region, the phononics analysis is needed to clarify how the folding affects the phonon transmission in the fold region. Based on Eq. 2, the phonon thermal conductivity can be calculated. Conceptually, there always exists discrepancy between the phonon thermal conductivity and the experimentally measured thermal conductivity, due to relaxation time approximation and the
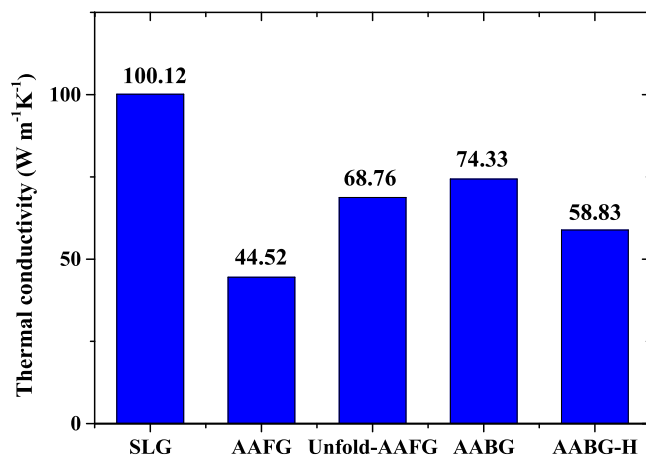


**Figure 3.** Thermal conductivities of SLG, AAFG, Unfold-AAFG, AABG, and AABG-H at 300 K.

neglected quantum effects in the classic MD simulations. Even so, that does not disturb the phononics analysis. Using the phonon group velocity and phonon lifetime in the Γ-K direction, the contribution of each branch to the total thermal conductivity can be calculated. Zou et al.[30] have reported the contribution of each branch of single-layer graphene to the total thermal conductivity. They find that the percentage of LA branch is 66.5%, that of TA branch is 28.6%, and that of ZA branch is 3.8% when AIREBO potential is used. For the purpose of verification, the phonon contribution to the thermal conductivity of SLG that contains $20 \times 20$ unit cells is calculated, and the result shows that the percentage of LA branch is 54.3%, that of TA branch is 34.6%, and that of ZA branch is 5.1%. Considering the statistical fluctuation, the calculated results in this work are almost the same as those in literature.

It should be noted that both the First-principle approach and the linearized Boltzmann transport equation (BTE) approach[31] have concluded that the ZA branches dominate the thermal transport in SLG. While in MD simulations the LA branches dominate the thermal transport in SLG. One reason of the discrepancy can be associated with the anomalously large Phonon density of states (PDOS) in BTE and the First-principle, which results in a large contribution to specific heat for ZA modes.

To analyze the effect of the folding, the thermal conductivity contributions of every phonon branch for AAFG, Unfold-AAFG, AABG, and AABG-H are calculated shown in Fig. 4. It can be determined that for the Unfold-AAFG, AABG, and AABG-H, the contribution of the LA phonon branch to the total thermal conductivity is about 55% ∼ 60%, and that of the TA phonon branch is about ∼30%, which is close to the results of the SLG. However, for AAFG, the contribution of the LA branch is 72.72%, and that of TA phonon branch is 18.34%. The contribution of TA phonons of AAFG to heat conduction, 18.34%, is smaller than that of the other three graphene's derived nanostructures. In contrast to SLG, Unfold-AAFG is hydrogenated at both ends in the $x$ direction and adopts free boundary conditions, but they do not affect the proportion of heat conduction contribution of each phonon branch. The phonon branch contributions of double-layer graphene AABG and AABG-H are also consistent to SLG, indicating that the two factors of hydrogenation passivation and bilayer structure rarely affect the contribution of phonon branches. On the other hand, when graphene is folded, the contribution of LA branch increases and the contribution of TA branch decreases, indicating that the folding can significantly change the proportion of TA branch and LA branch to heat conduction.

To further study the LA and TA branches of the AAFG, Unfold-AAFG, AABG, AABG-H, their phonon thermal conductivities of the LA and TA branches are shown in Fig. 5. All the thermal conductivity of the LA branches is located in the range of 32 ∼
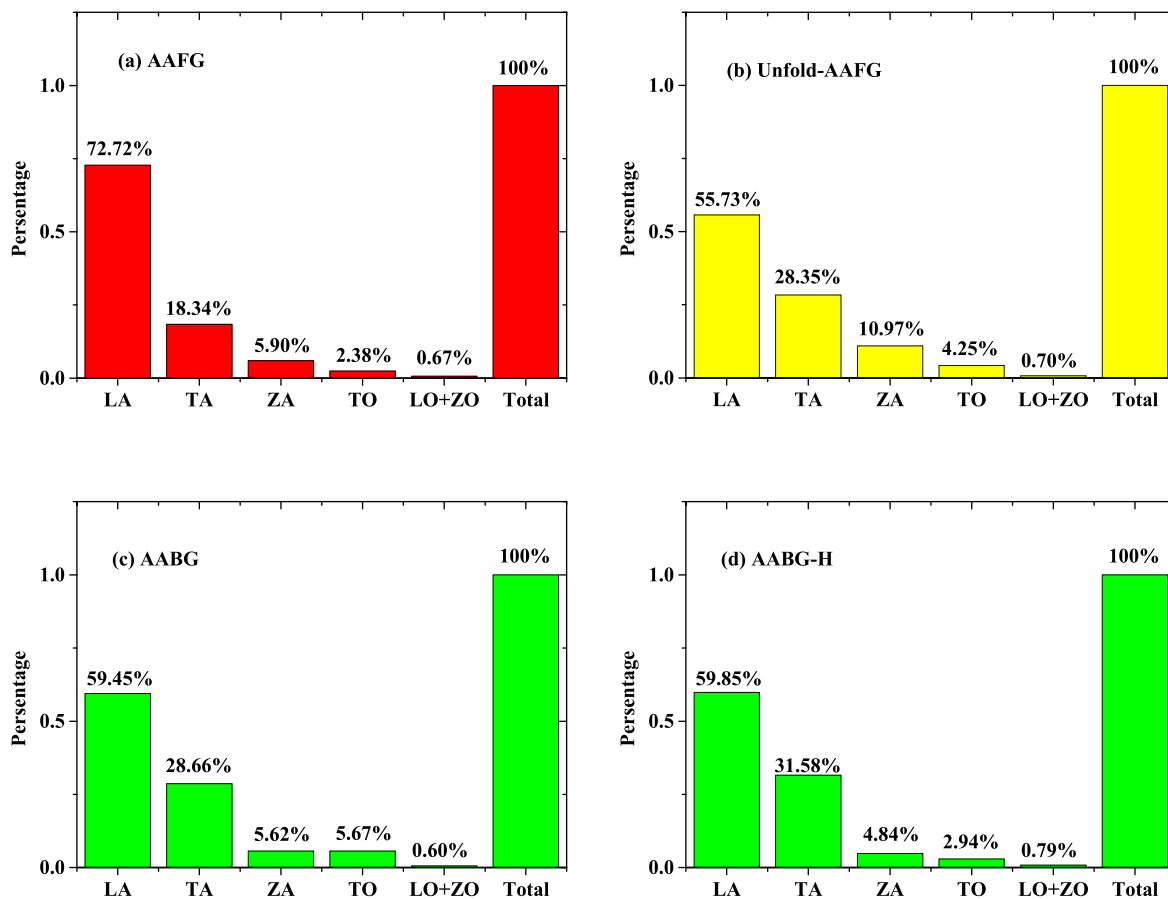
**Figure 4.** The thermal conductivity of each phonon branch as a percentage of the total thermal conductivity of (a) AAFG, (b) Unfold-AAFG, (c) AABG and (d) AABG-H at 300 K.
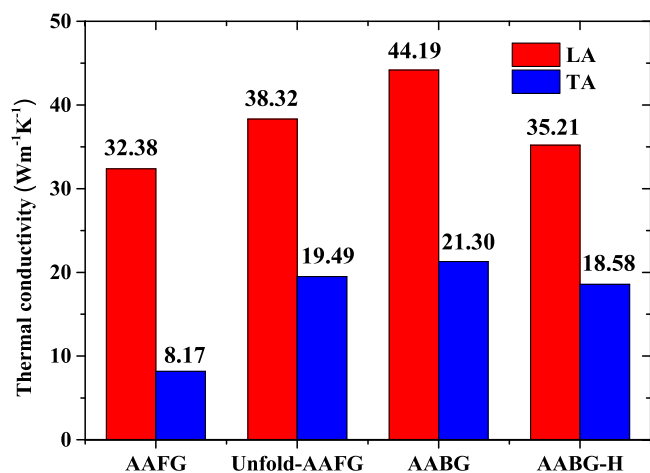


**Figure 5.** Thermal conductivity of LA branch and TA branch of AAFG, Unfold-AAFG, AABG, and AABG-H at 300 K.

45 W m$^{-1}$ K$^{-1}$, while the thermal conductivity of the TA branch of the AAFG is significantly lower than the other three TA branch thermal conductivities. For the unfold-AAFG, the thermal conductivity of LA branch of is 38.32 W m$^{-1}$ K$^{-1}$, and the thermal conductivity of TA branch is 19.49 W m$^{-1}$ K$^{-1}$. The ratio of TA branch thermal conductivity to LA branch thermal conductivity for the unfold-AAFG is 0.51. However, the ratio of TA to LA for AAFG is 0.25, which is much smaller than that of unfold-AAFG. It can be speculated that the thermal conductivity of LA branch is mainly reduced after folding. The contributions of the LA branches and TA branches of AABG and AABG-H are almost the same as those of the

SLG. Although the folded graphene also has a double-layered region, the results show that the double-layered structure rarely reduce the thermal conductivity of TA branch. Besides, the setting of initial conditions such as the hydrogenation and the free boundary conditions do not affect the contribution ratio of LA branch and TA branch to the phonon thermal conductivity. Therefore, it can be confirmed that the phonon thermal conductivity of TA branches is reduced by the folding.

In this work, the plane region of the AAFG and the bilayer graphene AABG are in the same size of 8.70 × 7.48 nm$^2$, and the stacking manner are both in AA-stacking. It is already known that the thermal conductivity of bilayer graphene is highly correlated to the in-plane size[32] and slightly affected by the stacking manner (AA- or AB-stacking).[33] In order to exclude the possibilities of the scale effect and the stacking manner effect, and make sure the folding can affect TA-phonon in the same way in folded graphene with various sizes and stacking manners, extra comparisons are carried out as follows. Two extra cases are set up compared with AAFG, one is AA-stacking folded graphene, denoted by AAFG2, whose size is 13.22 × 2.37 nm$^2$. While another one is AB-stacking folded graphene, denoted by ABFG, whose size is 8.70 × 7.48 nm$^2$, which is same as AAFG. As shown in Fig. 6, the contributions of LA branch and TA branch of them to the phonon thermal conductivity is almost consistent with that of AAFG discussed above. The contributions of their LA branches are both about 73%, and those of the TA branches are both about 18% ± 2%. Hence it can be confirmed that the folding structure certainly affects the contribution of TA branch to the thermal conductivity for folded graphene with various sizes and stacking manners.

***Phonon dispersion relationships.***—To understand the role of folding played in the phonon-folding scattering, phonon dispersion relationship and phonon lifetime will be discussed in this section.
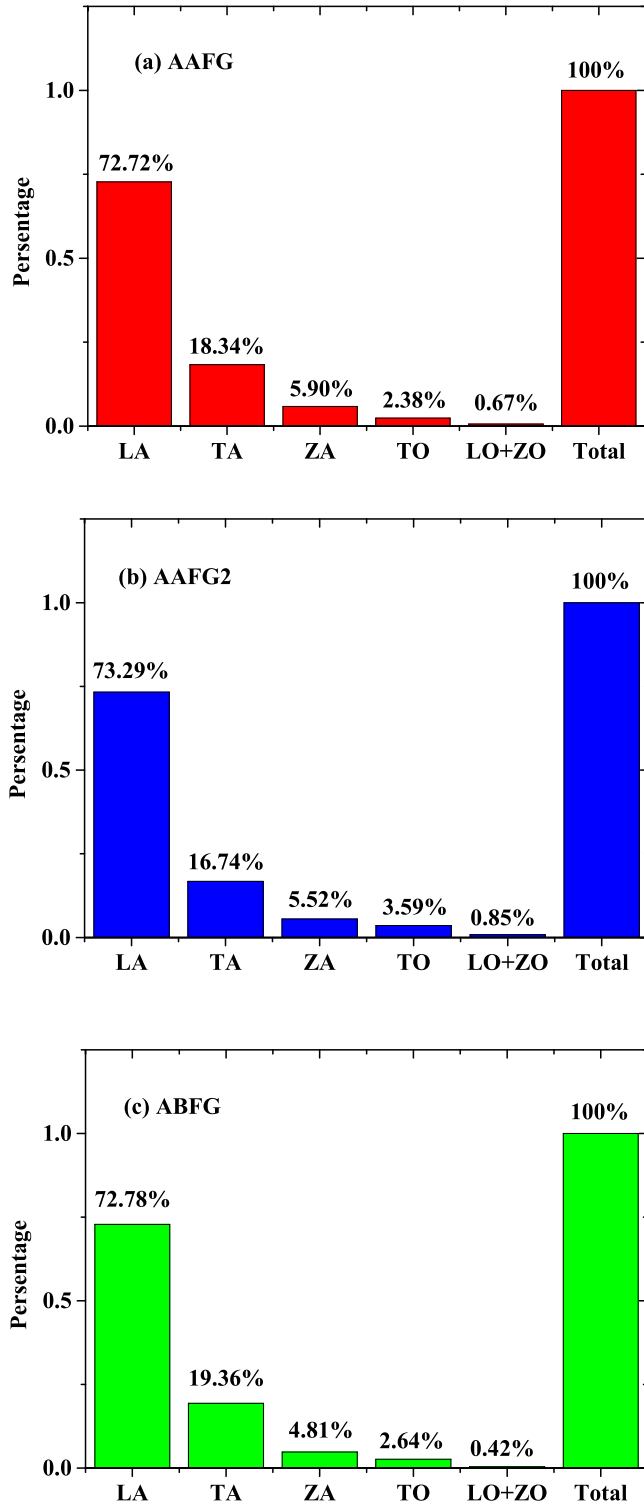
**Figure 6.** The thermal conductivity of each phonon branch as a percentage of the total thermal conductivity of (a) AAFG, (b) AAFG2 and (c)ABFG at 300 K.

Figure 7 presents the phonon dispersion curves of AAFG, Unfold-AAFG, AABG and AABG-H. The six phonon branches for all the cases can be distinctly observed. For all the cases, the relative locations of the branches and the amplitudes in the Γ points are basically the same, due to the same AIREBO potential is utilized to simulate all the inter-atomic forces. The same phonon branch trend indicates that the corresponding phonon group velocities are the same, which further illustrates that the folding rarely affect the

phonon group velocities of graphene. On the other hand, the different degrees of the dispersion in the dispersion curves demonstrate the difference between their phonon lifetimes. For the phonon branches of AABG (Fig. 7c), the curves are clearer and the dispersion is not apparent, predicting larger phonon lifetime. On contrary, the phonon branches of the other three, AAFG, Unfold-AAFG, and AABG-H, are broadened significantly, indicating the increasing phonon scattering and the shorter phonon lifetimes. The TA branch of AAFG (Fig. 7a) is more blurred than the other three TA branches, and the intersection of the TA branch and the ZO branch for AAFG is more chaotic. It can be figured out that the phonon lifetime of TA branch of AAFG should be smaller, which is the phononics explanation of the lower contribution of the TA branch for AAFG (Fig. 4).

To further substantiate this conclusion, the lifetime of TA branches and LA branches of the AAFG, Unfold-AAFG, AABG, and AABG-H are calculated using the Lorentzian function (Eq. 4). As shown in Fig. 8, the average TA-phonon lifetimes of AAFG, Unfold-AAFG, AABG, and AABG-H are 4.27 ps, 7.57 ps, 10.16 ps, and 7.43 ps, respectively. It can be found that the TA branch lifetime of AAFG is generally lower than the other three. A lower lifetime means increased phonon scattering and declined thermal conductivity. Therefore, the enhanced TA branch phonon scattering of AAFG is the main reason for the decline in thermal conductivity. The LA-phonon lifetimes tend to decrease with increasing frequency, and that of AAFG is not much different from the other three ones, indicating that the folding will not affect the LA-phonon, which explains that the phonon thermal conductivity of the LA branch of AAFG is basically the same as that of the others.

It is worth noting that in the dispersion curve of AABG, the ZA branch is clearly divided into two parts at low frequency near the Γ point, and then merges into one branch at high frequency, as shown in Fig. 7c. Kong et al.[34] have denoted this extra branch as ZO′, and the reason for the appearance of the ZO′ should be that the carbon atoms in the adjacent layers do not vibrate synchronously in $z$ direction. Apparently, the ZO′ branch should not exist in the dispersion curve of single-layer graphene. As shown in Fig. 7a, AAFG also has a ZO′ branch at low frequency, which indicates that the fold region will not affect the vibration of the two plane layers. Otherwise, the vibration of the upper and lower layers will still be asynchronous. Therefore, after graphene is folded, the plane region of the folded graphene will not be greatly affected. It should be only the fold region that reduces the phonon lifetime of TA branch. The fold region should be more stressed, which may limit the vibration of the carbon atoms. Besides, when phonons pass the fold, some phonons along the in-plane direction need to change from the in-plane into a mixed mode, and change back to an in-plane mode after passing the fold. This behavior is defined as the phonon mode mismatch.[7] Both of the factors that may affect the TA branch phonon transmission will be discussed in the next section.

***Stress contribution and phonon mode mismatch.***—The effects of stress contribution and phonon mode mismatch on the TA branch phonon transmission will be discussed. It should be noticed that there is the slight deformation caused by the fold stress between the fold region and the plain region, so that the size of the AAFG should be slightly different from that of AABG. The $x$-size of the AAFG is 8.61 nm, while the $x$-size of the AABG is 8.32 nm. The effect of the slight deformation caused by the fold stress is included in the analysis of the effect of the fold region on the phonon transmission.

In order to investigate the stress of the fold region, MD method is used to calculate the stress distribution of AAFG, Unfold-AAFG, AABG, and AABG-H. The stress tensor for atom $i$ is given by the following formula

$$S_{ab} = -mv_a v_b - W_{ab} \qquad [6]$$

where $a$ and $b$ taken on values $x$, $y$, $z$. The first term is a kinetic energy contribution for atom $i$, and the second term is the virial
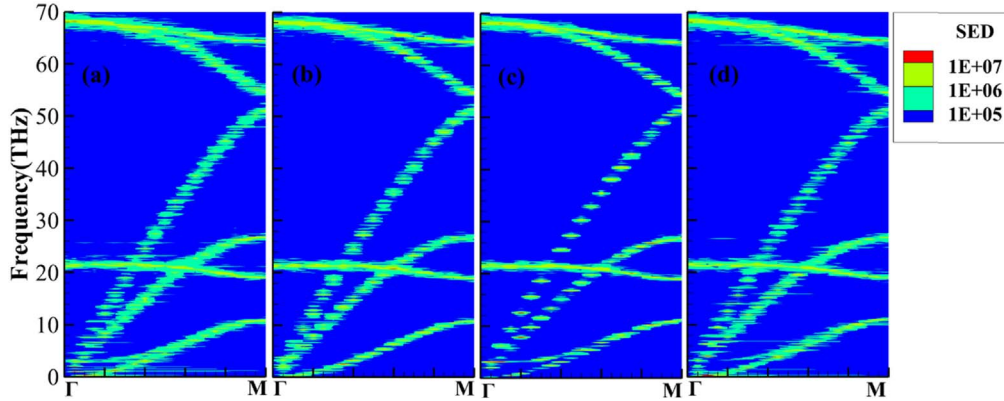
**Figure 7.** Phonon dispersion curves for different types of graphene, (a) AAFG, (b) Unfold-AAFG, (c) AABG, and (d) AABG-H.
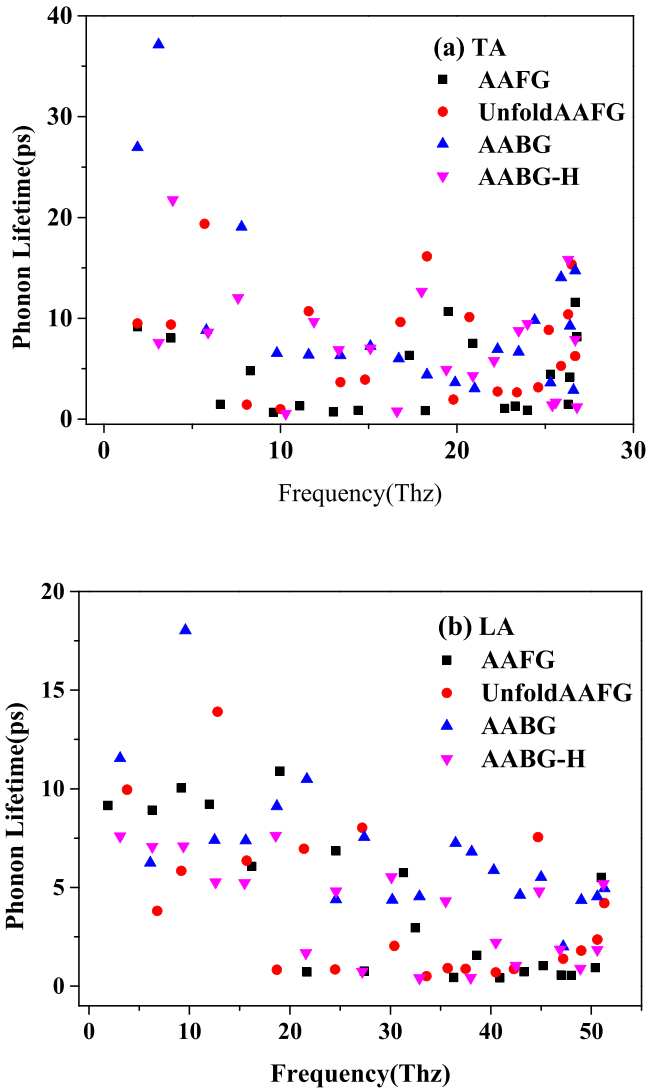


**Figure 8.** Phonon lifetimes of (a) TA branches and (b) LA branches of AAFG, Unfold-AAFG, AABG, and AABG-H.

contribution due to intra- and inter-molecular interactions, that is[35]

$$W(\mathbf{r}^N) = \sum_{i=1}^{N} \mathbf{r}_i \cdot \mathbf{F}_i \qquad [7]$$

where $\mathbf{r}^N$ is the instantaneous atom position, $\mathbf{r}^N = \mathbf{r}_1, \mathbf{r}_2, ..., \mathbf{r}_N$, and $\mathbf{F}_i$ is the total force acting on the atom $i$ due to interactions with other

atoms. Note that as defined in the formula, the per-atom stress is negative, and is actually a stress × volume formulation. As a result, if the per-atom stress are summed for atoms in the section and the sum is divided by $dV$, where $d$ is the dimension and $V$ is the volume of the section, the result of pressure should be $-P$, where $P$ is the total pressure of the section.[25] In this work, the system is cut into sections every 3 Å along the $x$ direction, where 3 Å is radius of semi-CNT region, and the pressure of each section can be calculated.

The results of the stress distributions are shown in Fig. 9. The left side of the AAFG is the fold region (Fig. 9a), where the compressive stress can be found. The right side is the H-terminated free edge, and the tensile stress is discovered. The uniform stress distribution in the middle of the AAFG is basically consistent with that of AABG. The ends of the unfold-AAFG are H-terminated free edge, so that both sides show the tensile stresses. It should be reminded that the TA branch of the unfold-AAFG is not affected, hence, similarly, the tensile force on the right side of AAFG should be rarely related to the decline of the phonon thermal conductivity of TA branch. The largest compressive stress exists in the fold region, whose maximum value is only about 0.08 GPa. Wei et al.[36] have found that it needs about 20 GPa to change the carbon-carbon bond length from 1.42 Å to 1.44 Å. In this work, such a compressive stress caused by the folding is too small to change the carbon-carbon interatomic microstructure. Hence it can be speculated that the effects of stress on the TA branch phonon transmission and the thermal conductivity are negligible.

Let the discussion go to the phonon mode mismatch behavior. It has been known that the phonon mean free path (MFP) is always larger in SLG (100 ~ 600 nm) than the size of the nana-scale SLG, so that the phonon transport in graphene can be affected by its structure. When there is more than one factor limiting the phonon MFP simultaneously, the total phonon scattering event can be described by the Matthiessen rule,[37] as

$$\tau_s^{-1} = \sum_i \tau_i^{-1} \qquad [8]$$

where $\tau_s$ is the lifetime of the total scattering event, and $\tau_i$ is the lifetime of the $i$ scattering process. In the folded graphene, the total scattering event includes intrinsic an-harmonic phonon-phonon scattering, boundary scattering, and phonon-folding scattering. It is reasonable to assume that these scatterings are independent of each other for nano-scale graphene.[38] In Fig. 8a, it can be found that the TA branch lifetime of AAFG is generally lower than that of the Unfold-AAFG. It can be speculated that, once the assumption stands, the additional phonon-folding scattering in AAFG is responsible for the reduced lifetime. When phonons pass the fold, some phonons along the in-plane direction need to change from the in-plane mode into a mixed mode, and change back to an in-plane mode after passing the fold. It will induce in-plane phonon scattering to redistribute the phonon energy to allow phonons to pass through the fold.
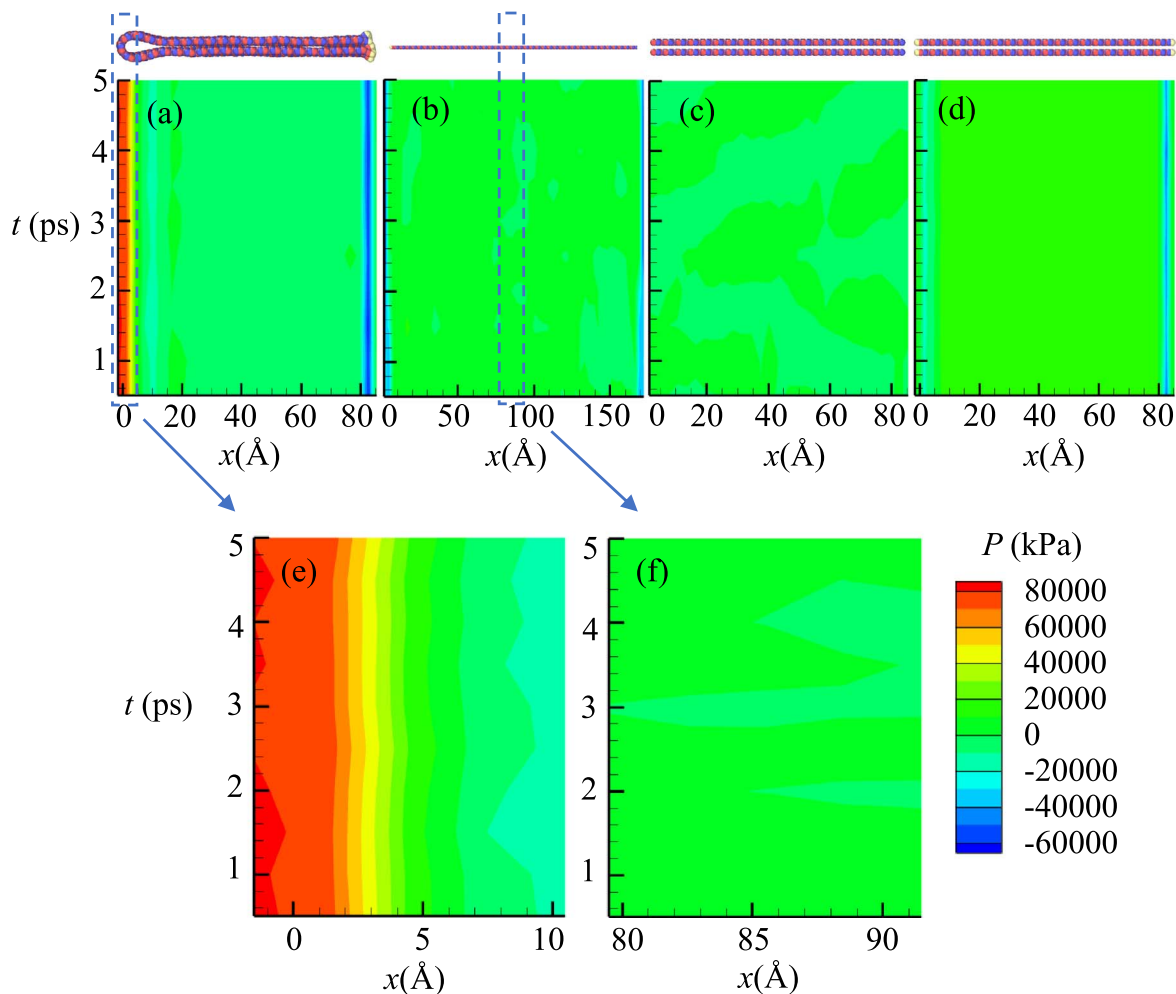
**Figure 9.** Stress distributions of different types of graphene, (a) AAFG, (b) Unfold-AAFG, (c) AABG, and (d) AABG-H, as well as the local stress distributions of (e) fold region in AAFG and (f) middle region in unfolded AAFG.

## Conclusions

This work utilizes the MD simulation approach to compare the thermal conductivities of graphene before and after folding. The contribution of each phonon branch to heat conduction are analyzed. The mechanism of the decline of the thermal conductivity for the folded graphene are discussed, and the phonon dispersion relationship and the phonon lifetime are calculated to understand the effect of the fold on phonon transmission. The conclusions of this work are as follows.

(1) The results show that the thermal conductivity of the folded graphene is 64.42% of that of the single-layer graphene before folding. Moreover, it can be found that the phonon thermal conductivity of TA branch will be apparently reduced after graphene is folded, leading to a significant decrease in the contribution of TA-phonon to heat conduction.

(2) Based on the SED analysis, the lifetime of TA branch in folded graphene is lower than that before folding, which is the main reason for the decrease of thermal conductivity. By evaluating the effects of the stress contribution and phonon mode mismatch behavior, it is found that the effects of stress on the TA branch phonon transmission and the thermal conductivity are negligible. While phonon-folding scattering should be responsible for the reduced lifetime and the decreasing thermal conductivity for folded graphene, which means that when passing the fold some phonons along the in-plane direction need to change from the in-plane mode into a mixed mode, and change back to an in-plane mode after passing the fold.

(3) The conclusions of this work reveal the mechanism of reduced thermal conductivity of folded graphene from a completely new perspective, and provide a new idea for precisely regulating the thermal conductivity of the TCM devices.

## ORCID

Xiao-Dong Wang ⓘ https://orcid.org/0000-0002-4533-6734

## References

1. A. K. Geim, "Graphene: status and prospects." *Scince*, **324**, 1530 (2009).
2. E. Y. Choi, S. Lee, and C. K. Kim, "Hybridization effects of nitrogen-doped graphene-carbon nanotubes and nano-onion carbons on the electrocatalytic activity of the oxygen reduction reaction." *ECS J. Solid State Sci. Technol.*, **7**, M128 (2018).
3. K. Spyrou, D. Gournis, and P. Rudolf, "Hydrogen storage in graphene-based materials: efforts towards enhanced hydrogen absorption." *ECS J. Solid State Sci. Technol.*, **2**, M3160 (2013).
4. C. Lee, X. Wei, J. W. Kysar, and J. Hone, "Measurement of the elastic properties and intrinsic strength of monolayer graphene." *Scince*, **321**, 385 (2008).
5. A. A. Balandin, S. Ghosh, W. Bao, I. Calizo, D. Teweldebrhan, F. Miao, and C. N. Lau, "Superior thermal conductivity of single-layer graphene." *Nano Lett.*, **8**, 902 (2008).

6. X. Yu, B. G. Zhang, S. Zhao, Z. X. Kao, S. H. Yang, and X. Y. Liu, "Enhancement of heat dissipation in LED using graphene and carbon nanotubes." *ECS J. Solid State Sci. Technol.*, **7**, M153 (2018).
7. Q. Song, M. An, X. Chen, Z. Peng, and N. Yang, "The adjustable thermal resistor by reversibly folding a graphene sheet." *Nanoscale*, **8**, 14943 (2016).
8. T. Ouyang, Y. Chen, Y. Xie, G. M. Stocks, and J. Zhong, "Thermal conductance modulator based on folded graphene nanoribbons." *Appl. Phys. Lett.*, **99**, 233101 (2011).
9. F. Hao, D. Fang, and Z. Xu, "Mechanical and thermal transport properties of graphene with defects." *Appl. Phys. Lett.*, **99**, 041901 (2011).
10. H. Yang, Y. Tang, Y. Liu, X. Yu, and P. Yang, "Thermal conductivity of graphene nanoribbons with defects and nitrogen doping." *Reactive & Functional Polymers*, **79**, 29 (2014).
11. H. C. Schniepp, J. L. Li, M. J. Mcallister, H. Sai, M. Herrera-Alonso, D. H. Adamson, R. K. Prud'homme, R. Car, D. A. Saville, and I. A. Aksay, "Functionalized single graphene sheets derived from splitting graphite oxide." *J. Phys. Chem. B*, **110**, 8535 (2006).
12. W. J. Evans, L. Hu, and P. Keblinski, "Thermal conductivity of graphene ribbons from equilibrium molecular dynamics: effect of ribbon width, edge roughness, and hydrogen termination." *Appl. Phys. Lett.*, **96**, 203112 (2010).
13. S.-P. Ju, K. Y. Chen, M. C. Lin, and Y. Ray, "Investigation of the thermal behaviors of folded graphene by non-equilibrium molecular dynamics simulation." *Carbon*, **77**, 36 (2014).
14. W. J. Yin, Y. E. Xie, L. M. Liu, Y. P. Chen, R. Z. Wang, X. L. Wei, J. X. Zhong, and L. Lau, "Atomic structure and electronic properties of folded graphene nanoribbons: a first-principles study." *J. Appl. Phys.*, **113**, 173506 (2013).
15. S. L. Chang, B. R. Wu, P. H. Yang, and M. F. Lin, "Geometric, magnetic and electronic properties of folded graphene nanoribbons." *RSC Adv.*, **6**, 64852 (2016).
16. N. Yang, X. Ni, J.-W. Jiang, and B. Li, "How does folding modulate thermal conductivity of graphene?" *Appl. Phys. Lett.*, **100**, 093107 (2012).
17. J. Zang, S. Ryu, N. Pugno, Q. Wang, Q. Tu, M. J. Buehler, and X. Zhao, "Multifunctionality and control of the crumpling and unfolding of large-area graphene." *Nat. Mater.*, **12**, 321 (2013).
18. R. Murali, Y. Yang, K. Brenner, T. Beck, and J. D. Meindl, "Breakdown current density of graphene nanoribbons." *Appl. Phys. Lett.*, **94**, 243114 (2009).
19. C. Yu and G. Zhang, "Impacts of length and geometry deformation on thermal conductivity of graphene nanoribbons." *J. Appl. Phys.*, **113**, 044306 (2013).
20. C. Wang, Y. Liu, L. Li, and H. Tan, "Anisotropic thermal conductivity of graphene wrinkles." *Nanoscale*, **6**, 5703 (2014).
21. A. Cao and J. Qu, "Size dependent thermal conductivity of single-walled carbon nanotubes." *J. Appl. Phys.*, **112**, 013503 (2012).
22. X. Li, J. Chen, C. Yu, and G. Zhang, "Comparison of isotope effects on thermal conductivity of graphene nanoribbons and carbon nanotubes." *Appl. Phys. Lett.*, **103**, 013111 (2013).
23. H. Zhang, T. Zhou, G. Xie, J. Cao, and Z. Yang, "Thermal transport in folded zigzag and armchair graphene nanoribbons." *Appl. Phys. Lett.*, **104**, 241908 (2014).
24. J. E. Turney, E. S. Landry, A. J. H. McGaughey, and C. H. Amon, "Predicting phonon properties and thermal conductivity from anharmonic lattice dynamics calculations and molecular dynamics simulations." *Physical Review B*, **79**, 064301 (2009).
25. S. Plimpton, "Fast parallel algorithms for short-range molecular dynamics." *J. Comput. Phys.*, **117**, 1 (1995).
26. S. J. Stuart, A. B. Tutein, and J. A. Harrison, "A reactive potential for hydrocarbons with intermolecular interactions." *J. Chem. Phys.*, **112**, 6472 (2000).
27. J. A. Thomas, J. E. Turney, R. M. Iutzi, C. H. Amon, and A. J. McGaughey, "Predicting phonon dispersion relations and lifetimes from the spectral energy density." *Physical Review B*, **81**, 081411 (2010).
28. D. Nika, E. Pokatilov, A. Askerov, and A. Balandin, "Phonon thermal conduction in graphene: role of Umklapp and edge roughness scattering." *Physical Review B*, **79**, 155413 (2009).
29. S. Ghosh, W. Bao, D. L. Nika, S. Subrina, E. P. Pokatilov, C. N. Lau, and A. A. Balandin, "Dimensional crossover of thermal transport in few-layer graphene." *Nat. Mater.*, **9**, 555 (2010).
30. J. H. Zou, Z. Q. Ye, and B. Y. Cao, "Phonon thermal properties of graphene from molecular dynamics using different potentials." *J. Chem. Phys.*, **145**, 134705 (2016).
31. L. Lindsay, D. A. Broido, and N. Mingo, "Flexural phonons and thermal transport in graphene." *Physical Review B*, **82**, 115427 (2010).
32. H. Y. Cao, Z. X. Guo, H. Xiang, and X. G. Gong, "Layer and size dependence of thermal conductivity in multilayer graphene nanoribbons." *Phys. Lett. A*, **376**, 525 (2012).
33. Y. Liu, H. Yang, N. Liao, and P. Yang, "Investigation on thermal conductivity of bilayer graphene nanoribbons." *RSC Adv.*, **4**, 54474 (2014).
34. B. D. Kong, S. Paul, M. Buongiorno Nardelli, and K. W. Kim, "First-principles analysis of lattice thermal conductivity in monolayer and bilayer graphene." *Physical Review B*, **80**, 033406 (2009).
35. A. P. Thompson, S. J. Plimpton, and W. Mattson, "General formulation of pressure and stress tensor for arbitrary many-body interaction potentials under periodic boundary conditions." *J. Chem. Phys.*, **131**, 154107 (2009).
36. N. Wei, L. Xu, H. Q. Wan, and J. C. Zheng, "Strain engineering of thermal conductivity in graphene sheets and nanoribbons: a demonstration of magic flexibility." *Nanotechnology*, **22**, 105705 (2011).
37. K. E. Goodson and Y. S. Ju, "Heat conduction in novel electronic films." *Annu. Rev. Mater. Sci.*, **29**, 261 (1999).
38. M. Holland, "Analysis of lattice thermal conductivity." *Phys. Rev.*, **132**, 2461 (1963).